*Africa Journal of Physical Sciences Vol. 4, pp. 126-138, June 2020*
*http://journals.uonbi.ac.ke/index.php/ajps/index*
*ISSN 2313-3317*

# Application of GDGT-derived temperature proxies on Mt. Kenya

**OMUOMBO Christine[1,*], HUGUET Arnaud[2], WILLIAMSON David[3], OLAGO Daniel[1]**

[1]Department of Geology University of Nairobi, P.O Box 30197-00100, Nairobi, Kenya
[2] Sorbonne Université, CNRS, EPHE, PSL, UMR METIS, F-75005 Paris, France
[3]IRD Kenya, ICRAF, Box 30677-00100 Nairobi, Kenya

*Corresponding author email: omuombo@uonbi.ac.ke

ARTICLE INFO

*Article History:*
Submitted: 3 August 2019
Accepted: 19 Mar 2020
Available online: June 2020

*Keywords:*
Mount Kenya
GDGTs
TEX86
MBT/CBT
Paleoelevation

**ABSTRACT**

Glycerol dialkyl glycerol tetraethers (GDGTs) are membrane lipids produced by archaea (isoprenoid GDGTs - iGDGTs) and bacteria (branched GDGTs - brGDGTs) in terrestrial and aquatic settings. Our study examines the relationship between GDGT distribution and environmental parameters in soils collected along Mt. Kenya to examine their applicability as paleotemperature and paleoelevation proxies. Both global and regional calibrations were tested on our dataset. brGDGT-derived temperature for Mt. Kenya linearly correlates with altitude and is consistent for all the calibrations although the derived temperature lapse rate (0.53 °C/100 m) along the mountain from the global soil calibration by [1] is consistent with gridded climate data (0.52°C /100 m) along this transect. This lapse rate is lower than the regional estimate of 0.70°C /100 m previously obtained in other altitudinal gradients (Mt. Rungwe and Mt. Kilimanjaro) from the same region. Although brGDGTs are considered as a robust paleoelevation proxy regionally, individual site performances may be unique to their environmental setting, geographic location and altitude. In addition, a poor linear correlation between altitude and iGDGT-derived $TEX_{86,}$ a rarely investigated proxy in soils, implies that there are many other factors not investigated here that affects its applicability in tracking temperature changes along altitudinal transects.


ISSN 2313-3317

## 1. Introduction

Glycerol dialkyl glycerol tetraethers (GDGTs) are membrane lipids of both archaeal and bacterial origin containing two long alkyl chains attached to glycerol moieties at both ends. They are found in a wide range of environments such as marine and lacustrine sediments [2], [3], soils [1], [4], peatlands [5], [6], water columns [2], [7] and speleothems [8]. GDGTs exhibit a large diversity in their carbon skeletal compositions but two main classes have been identified, namely isoprenoid GDGTs (iGDGTs) and branched GDGTs (brGDGTs). Isoprenoid GDGTs (iGDGTs) are produced by archaea with structures differing by the number of cyclopentane moieties in the alkyl chains (from 0 to 4; see Figure 1). GDGT – 0 is sometimes referred to as caldarchaeol and is the most common iGDGT detected of the archaeal phyla [9] while crenarchaeol which consists of 4 cyclopentane rings with an additional cyclohexane moiety (Figure 1; [9], [10], [10] is thought to be specific to phylum *Thaumarchaeota* even though it has been suggested that it could be produced by Marine Group II *Euryarchaeota*. The crenarchaeol possesses a regio isomer (i.e. asymmetric carbon in the cyclohexane structure) called the crenarchaeol regio isomer that is present in significant amounts in natural samples [12].

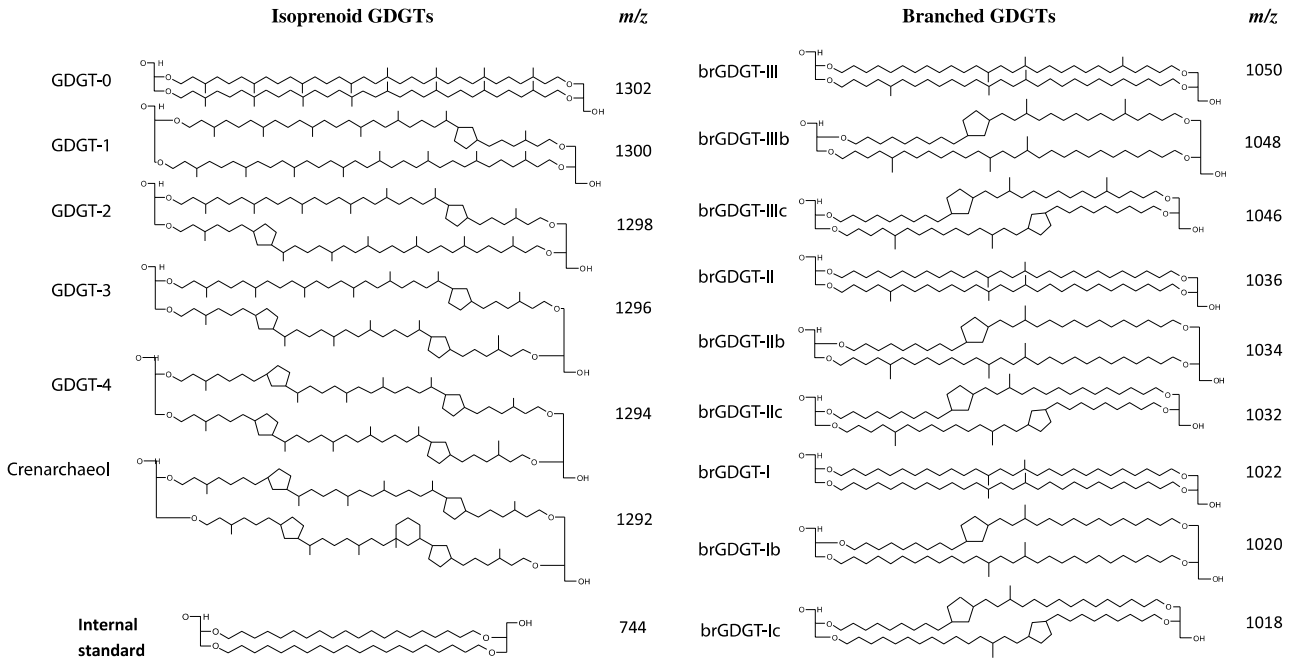


**Figure 1: Structures of isoprenoid GDGTs (iGDGTs) and branched (brGDGTs). iGDGT nomenclature (iGDGT-x) is derived from the presence of cyclopentyl moieties in the alkyl chains, where x represents the number of cyclopentane moieties. The structure of brGDGT displays the presence of the cyclopentane moieties, and a basic structure containing methyl (four to six) branches. IS represents the $C_{46}$ synthesized internal standard.**

In contrast to the iGDGTs, brGDGTs are lipids of bacterial origin whose stereoconfiguration from NMR characterisation is opposite to that of iGDGTs (Figure 1; [13]). Little is known about their sources and biosynthesis although they display a huge abundance in water logged areas such as peats hence the suggestion that they are produced by anaerobic bacteria [14]. Although more studies are needed to constrain the source of these micro-organisms *Acidobacteria* might be possible producers of the brGDGTs [14]. The ubiquity of brGDGTs in terrestrial environments has led to its utility in estimating catchment processes largely linked to soil organic matter presence in different environments. [15] developed a Branched to Isoprenoid Tetraether (BIT) Index to estimate terrestrial inputs into the aquatic environments. The index, based on the ratio of brGDGT and crenarchaeol, assumes that brGDGTs are produced exclusively by soil bacteria and crenarchaeol only by aquatic *Thaumarchaeota* [9] however, recent studies suggest that brGDGTs and crenarchaeol are also produced *in situ* in aquatic environments and soils respectively [3], [13], [16] challenging the applicability of this index.

The controlling factors that affect the relative abundance of the brGDGTs in soils was first investigated by [4] from 130 soils collected globally. These authors showed that structural differences in brGDGTs were found to correlate with pH and air temperature. The corresponding relationships were expressed as follows: (i) The average number of cyclopentyl moieties displays a positive correlation ($R^2$ = 0.70) with soil pH through the cyclization index of brGDGTs (CBT) and (ii) The number of methyl branches positively correlates ($R^2$ = 0.62) with Mean Annual Air Temperature (MAAT) and to a lesser extent with soil pH ($R^2$ = 0.37) through methylation of brGDGTs (MBT). In an aim to improve the accuracy of the MBT/CBT proxy [1] added 126 new soil surface samples to [17]

global dataset. This led to the development of a new calibration based on MBT' that excluded brGDGT-IIIb and brGDGT-IIIc (Figure 1) from the MBT relationship as they were frequently below the detection limit and comprised <1% of the total brGDGTs on average [1]. These relationships advanced the use of the brGDGTs as a paleoelevation proxy along different altitudinal transects [3], [18], [19] [20] [20].

Analytical uncertainties and discrepancies arising from the application of GDGT-derived proxies in the modern environments [22] [23] has led to the recognition that other environmental parameters than temperature/pH may also have an influence on GDGT distribution. The recent improvement in analytical separation of brGDGTs and subsequent detection of additional isomers of brGDGTs (with methyl groups at either position 5 or 6, referred to as 5- and 6-methyl brGDGT isomers) slightly improved the accuracy of temperature reconstruction based on these lipids [24]. The application of this new methodology on previous samples from the global datasets of [1] and [17] have shown that the fractional abundance of the 6-methyl brGDGTs is highly correlated to pH and thus the source of pH dependence of the MBT' [24]. This led to the exclusion the 6-methyl isomers from the MBT' allowing a reconstruction of MAAT based only on 5-methyl brGDGTs which is not influenced by pH [24]. Although we acknowledge the interest of this new analytical method for the separation of brGDGT isomers, iGDGTs and brGDGTs in our samples were analysed using the original method based on cyano column [1].

In East Africa, a regional calibration between MBT/CBT and mean annual air temperature (MAAT) was developed by [25] using soil samples collected along Mt. Rwenzori (Uganda; Loomis et al. 2011), Mt. Rungwe (Tanzania; [20]), Mt. Kilimanjaro (Tanzania; [18]) and Mt. Kenya (Kenya). This calibration improved both the strength of the correlation ($R^2$ 0.77) and the accuracy of the MAAT reconstruction (Root Mean Square Error – RMSE – 2.4 °C) compared to the global soil calibration by [1] ($R^2$ 0.56 and RMSE 4.2 °C). This is likely due to the fact that regional environmental parameters such as the physical and chemical soil properties or the precipitation regime affect the performance of the reconstructions. In any case, this study showed the robustness of the MBT/CBT proxy in East Africa.

In this study, the concentration and relative distribution of brGDGTs and iGDGTs were determined in soils collected along the north eastern slopes of Mt. Kenya between 1800 m asl and 3268 m asl (Figure 2). Located at the equator, the mountain exhibits a wide range of ecological and climatic zones based on the changes in rainfall and elevation [26], [27]. Precipitation on the mountain increases with altitude until about 2500 m asl above which a decline in the amount of rainfall is observed similar to other East African Mountains [26], [28]. A decline in temperature from the foothills to the nival zone is observed with diurnal daily variations [29]. Although there are no marked seasonal temperature variations a strong altitudinal gradient of up to 1°C per 100 m has been suggested [29], [30]. The aim of this study is to investigate the applicability of the MBT/CBT and $TEX_{86}$ indices as distinct and complimentary paleotemperature and paleoelevation proxies on the mountain.

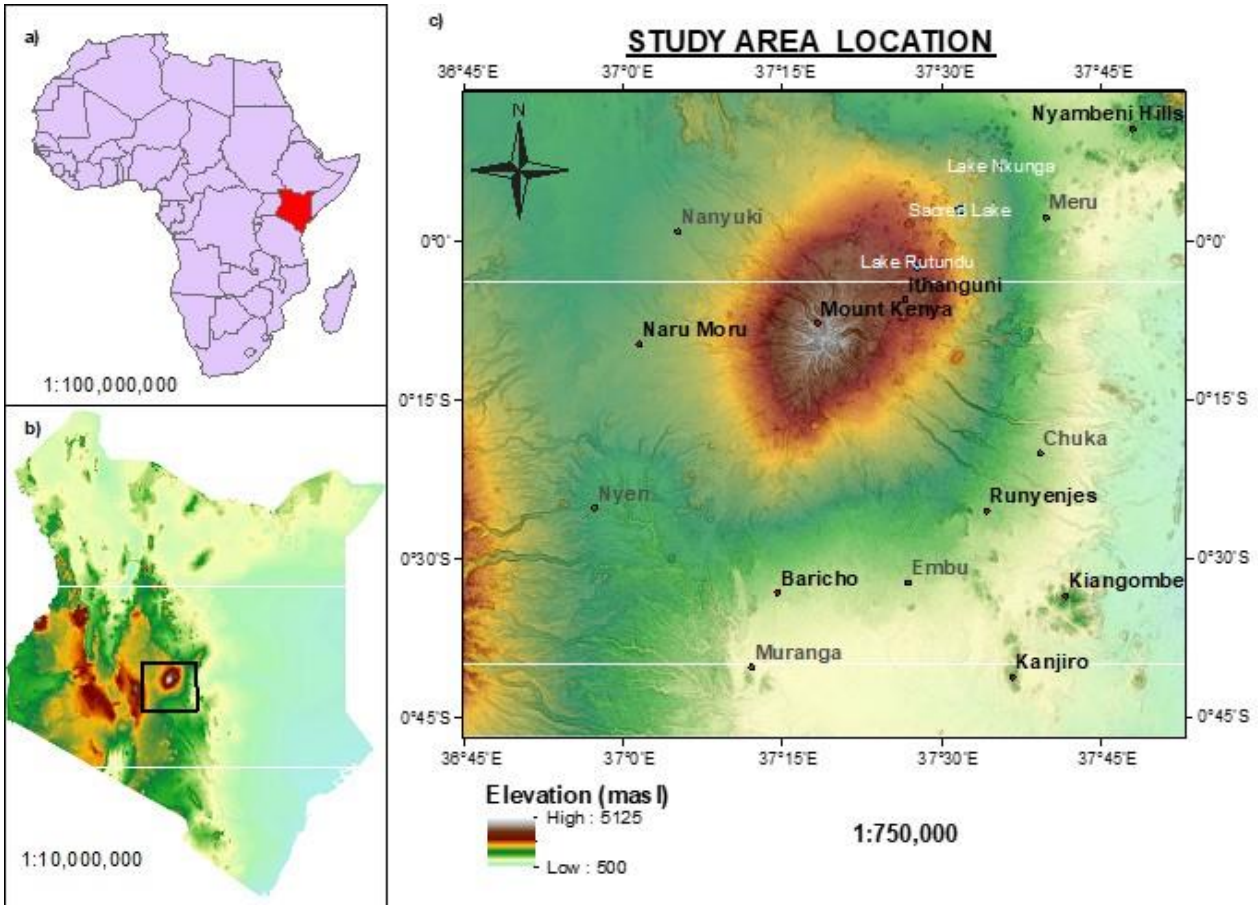


**Figure 2: Maps showing the location of Mt. Kenya in Kenya (a,b) and the study area on the north-eastern flanks of Mount Kenya.**

## 2. Materials and Methods

### *2.1 Sample collection*

27 surface soil samples (within the upper surface 0-5cm) were collected during two field campaigns carried out in 2011 and 2013 along an altitudinal transect (1800 m – 3268 m asl) on the North Eastern slopes of Mt. Kenya (Figure 2; **Error! Reference source not found.**). These samples were preserved in resealable plastic bags and initially stored in the cold room at the University of Nairobi and the soil storage facility at ICRAF Soil and Plant laboratories at 4.0 °C for 2 weeks after which they were transported to the IRD laboratory in Bondy, France in 2011 and METIS laboratory in Sorbonne Université, Paris, France.

### *2.2 Sample preparation*

For each sample, twenty grams of soils were oven dried at 40°C for 48hrs and then extracted by Accelerated Solvent Extraction (Dionex ASE 100, ThermoFisher) using a 9:1 dichloromethane/methanol solvent mixture [20]. Each sample was extracted three times at 100°C and under 100 bar pressure. The extracted lipids were dried under vacuum using a rotary evaporator in a water bath maintained at room temperature. The separation of the total lipid extracts into polar and apolar fractions was carried out using a column filled with activated $Al_2O_3$ (put in the oven at 150°C for two hours before use). The elution was performed with two mixtures of solvents: *n*-heptane: DCM (9:1, v/v) for the apolar fraction and DCM:MeOH (1:1, v/v) for the polar fraction. The separated fractions were dried by rotary evaporation. These samples were transferred to four ml vials using DCM, after which they were dried under $N_2$ gas and dissolved in 1 mL hexane prior to

analysis.

**Table 1: Sample information (Sample No, Altitude and coordinates), the total organic carbon content (% Corg) and relative abundances of the total GDGTs total (μg/g) and relative (%) GDGTs.**

| No. | Altitude (m asl) | Coordinates | | Corg (%) | brGDGT μg/g Corg | iGDGT μg/g Corg | brGDGT (%) | iGDGT (%) |
|---|---|---|---|---|---|---|---|---|
| 1 | 1800 | -0.82 | 36.97 | 2.1 | 5.85 | 1.21 | 82.9 | 17.1 |
| 2 | 1800 | -0.82 | 36.97 | 3.1 | 15.10 | 1.59 | 90.5 | 9.5 |
| 3 | 1823 | 0.11 | 37.60 | 3.6 | 4.06 | 0.95 | 81.0 | 19.0 |
| 4 | 1847 | 0.11 | 37.59 | 21.4 | 7.68 | 1.57 | 83.0 | 17.0 |
| 5 | 1847 | 0.11 | 37.59 | 4.4 | 8.15 | 1.47 | 84.7 | 15.3 |
| 6 | 1847 | 0.11 | 37.59 | 4.7 | 3.79 | 1.01 | 79.0 | 21.0 |
| 7 | 1897 | 0.04 | 37.60 | 2.6 | 8.34 | 0.99 | 89.4 | 10.6 |
| 8 | 2027 | 0.04 | 37.58 | 3.2 | 8.76 | 0.34 | 96.3 | 3.7 |
| 9 | 2052 | 0.14 | 37.48 | 1.3 | 7.24 | 1.71 | 80.9 | 19.1 |
| 10 | 2097 | 0.14 | 37.47 | 1.4 | 4.86 | 1.09 | 81.7 | 18.3 |
| 11 | 2130 | 0.04 | 37.56 | 2.8 | 6.16 | 0.66 | 90.4 | 9.6 |
| 12 | 2189 | 0.13 | 37.46 | 2.7 | 5.28 | 1.98 | 72.7 | 27.3 |
| 13 | 2258 | 0.03 | 37.55 | 2.0 | 2.37 | 0.26 | 90.2 | 9.8 |
| 14 | 2318 | 0.04 | 37.54 | 4.3 | 4.14 | 0.08 | 98.1 | 1.9 |
| 15 | 2323 | 0.12 | 37.45 | 1.2 | 4.66 | 3.52 | 57.0 | 43.0 |
| 16 | 2350 | 0.05 | 37.53 | 15.2 | 11.11 | 0.54 | 95.4 | 4.6 |
| 17 | 2500 | 0.08 | 37.48 | 5.4 | 2.93 | 0.65 | 81.9 | 18.1 |
| 18 | 2642 | 0.06 | 37.47 | 20.0 | 15.79 | 0.70 | 95.8 | 4.2 |
| 19 | 2705 | 0.06 | 37.46 | 12.0 | 4.95 | 1.31 | 79.1 | 20.9 |
| 20 | 2846 | 0.05 | 37.45 | 26.3 | 6.95 | 0.53 | 93.0 | 7.0 |
| 21 | 2924 | 0.05 | 37.43 | 27.8 | 4.74 | 0.04 | 99.1 | 0.9 |
| 22 | 3047 | 0.02 | 37.42 | 11.2 | 11.49 | 0.87 | 92.9 | 7.1 |
| 23 | 3119 | -0.04 | 37.46 | 7.0 | 4.08 | 0.03 | 99.2 | 0.8 |
| 24 | 3119 | -0.04 | 37.46 | 14.2 | 6.64 | 0.02 | 99.7 | 0.3 |
| 25 | 3119 | -0.04 | 37.46 | 7.0 | 14.91 | 0.12 | 99.2 | 0.8 |
| 26 | 3160 | -0.01 | 37.42 | 8.9 | 2.60 | 0.54 | 82.7 | 17.3 |
| 27 | 3268 | -0.04 | 37.44 | 10.7 | 2.97 | 0.07 | 97.8 | 2.2 |

### *2.3 Sample analysis*

GDGTs were analysed by high-performance liquid chromatography coupled to mass spectrometry (HPLC-MS) using an Agilent 1100 series HPLC instrument equipped with an automatic injector and coupled to a PE Sciex API 3000 mass spectrometer [20]. Separation was achieved with a Prevail Cyano column (2.1 mm x 150 mm, 3 µm; Alltech, Deerfield, IL, USA) at 30°C, using a mixture of A and B (A= hexane and B= isopropanol) at 0.2 ml/min. Elution began at 99% A/1% B for 5 min followed by a linear gradient to 98% A/2% B in 45 min. A second linear gradient led to a mixture of 90 % A/10 % B in 10 min, maintained for 10 min and returned to the initial conditions (99% A/1% B) in 14 min, then maintained for 10 min. The injection volume was 10 µl. Ionization was performed with an Atmospheric Pressure Chemical Ionization Source (APCI). Single ion monitoring (SIM) of the $[M+H]^+$ ions were used to detect the GDGTs [20]. Semi-quantification of the GDGTs was performed by comparing the integrated signal of the respective compound with the signal of a $C_{46}$ synthesized

internal standard, as described by [31]. It should be noted that the brGDGT data of Mt. Kenya soils reported in this study were included in the regional East African calibration previously published by [25].

The MBT and CBT indices were calculated according to the equations developed by [17]:

$$MBT= ([I+Ib+Ic])/([III+IIIb+IIIc]+[II+IIb+IIc]+[I+Ib+Ic]) \quad [Eq. 1]$$

$$CBT= -\log([Ib+IIb])/([I+II]) \quad [Eq. 2]$$

Roman numbers refer to the GDGT structures described in Figure 1.

The MBT' was calculated as follows [1]:

$$MBT'= ([I+Ib+Ic])/([III]+[II+IIb+IIc]+[I+Ib+Ic]) \quad [Eq. 3]$$

MAAT was estimated using the global soil calibration developed by [17]; Eq. 4 and the extended calibration introduced by [1]; Eq. 5 and the regional calibration by [25]; Eq. 6 respectively.

$$MAAT= (MBT-0.122-0.187\times CBT)/0.020 \quad [Eq. 4]$$

$$MAAT=0.81-5.67 \times CBT+31.0 \times MBT' \quad [Eq. 5]$$

$$MAAT=-8.17 \times CBT + 25.39 \times MBT + 9.14 \quad [Eq. 6]$$

pH was calculated using soil calibrations developed by [17]]; Eq. 7 and [[1]]; Eq. 8:

$$pH= (3.33-CBT)/0.38 \quad [Eq. 7]$$

$$pH=7.90-1.97 \times CBT \quad [Eq. 8]$$

The BIT index was calculated as follows ([15]; Eq. 9):

$$BIT= (I+II+III)/(I+II+III+Crenachaeol) \quad [Eq. 9]$$

$TEX_{86}$ was calculated as follows ([12]; Eq. 10):

$$TEX_{86}=(GDGT\ 2+GDGT3+Crenachaeol)/(GDGT1+GDGT2+GDGT3+Crenarchaeol') \quad [Eq. 10]$$

*Crenarchaeol' refers to the regio isomer of this compound.*

## 3. Results and Interpretation

### *3.1 GDGT distribution and concentrations*

BrGDGTs and iGDGTs were detected in all the soil samples collected along the transect (**Error! Reference source not found.**). Generally, the brGDGTs are more abundant than the iGDGTs comprising of 57.0 to 99.7% of the total GDGTs (i.e. brGDGTs + iGDGTs). The relative abundance of iGDGTs ranges from 0.3 to 43.0% with an average of 12.1% of the total GDGTs, consistent with the average relative abundances (10 %) reported by [13] for soils from all over the world. The total brGDGT concentrations in the soils range from 2.4 to 15.8 µg/g $C_{org}$ (mean: 6.87 µg/g $C_{org}$) (Table 1). These values agree with the abundances of brGDGTs previously reported in soil samples from East Africa ranging from 1.1 to 8.3 µg/g $C_{org}$ for Mt. Rungwe, Tanzania [20] and of 4.0 and 20 µg/g $C_{org}$ for soils from Western Uganda [32]. The iGDGT concentration ranges from 0.002 to 0.352 µg/g $C_{org}$ (mean: 0.088 µg/g $C_{org}$) of dry soil weight, consistent with the regional ranges previously reported as 0.05 and 1.5 µg/g $C_{org}$ in Mt. Rungwe Tanzania [20].

**Table 2: The relative abundance of branched and isoprenoid GDGTs in the soil samples**

| No. | Altitude (m asl) | Relative Branched GDGTs (%) | | | | | | | | | Relative Isoprenoid GDGTs (%) | | | | | | |
|---|---|---|---|---|---|---|---|---|---|---|---|---|---|---|---|---|---|
| | | I | Ib | Ic | II | IIb | IIc | III | IIIb | IIIc | 0 | 1 | 2 | 3 | 4 | Cren | Cren' |
| 1 | 1800 | 74.4 | 1.7 | n.d | 23.5 | 0.5 | n.d | n.d | n.d | n.d | 20.3 | 23.4 | 22.0 | 13.2 | n.d | 15.1 | 5.9 |
| 2 | 1800 | 63.6 | 3.9 | 0.2 | 28.4 | 1.3 | n.d | 2.6 | n.d | n.d | n.d | n.d | 20.0 | 12.2 | 19.5 | 39.3 | 9.0 |
| 3 | 1823 | 54.5 | 14.1 | 6.3 | 16.7 | 5.6 | 0.3 | 2.5 | n.d | n.d | 12.9 | 4.7 | n.d | n.d | 16.9 | 57.5 | 8.0 |
| 4 | 1847 | 39.6 | 14.0 | 4.0 | 30.2 | 6.3 | 1.1 | 4.8 | n.d | n.d | 18.8 | 8.2 | 10.7 | 8.7 | n.d | 45.4 | 8.2 |
| 5 | 1847 | 64.7 | 3.1 | 1.3 | 27.1 | 1.3 | 0.4 | 2.1 | n.d | n.d | 21.2 | 5.3 | 14.4 | 6.7 | n.d | 45.7 | 6.7 |
| 6 | 1847 | 35.4 | 13.9 | 3.7 | 33.9 | 8.0 | 1.2 | 3.9 | n.d | n.d | n.d | n.d | 10.4 | 6.1 | 17.1 | 53.2 | 13.2 |
| 7 | 1897 | 63.0 | 5.7 | 2.0 | 24.5 | 2.0 | 0.5 | 2.3 | n.d | n.d | 23.8 | 8.6 | 10.7 | 7.4 | n.d | 42.6 | 7.0 |
| 8 | 2027 | 40.9 | 6.8 | 1.1 | 39.9 | 4.1 | 0.8 | 6.3 | n.d | n.d | 32.1 | 9.5 | 7.8 | 3.9 | n.d | 39.6 | 7.1 |
| 9 | 2052 | 59.0 | 4.2 | 0.8 | 29.5 | 1.8 | 0.3 | 3.8 | 0.6 | n.d | 63.8 | 4.6 | 6.1 | 2.3 | n.d | 20.5 | 2.7 |
| 10 | 2097 | 43.3 | 6.0 | 1.5 | 37.0 | 5.3 | 0.7 | 6.1 | 0.2 | n.d | 20.1 | 9.1 | 13.6 | 6.8 | n.d | 45.1 | 5.3 |
| 11 | 2130 | 35.9 | 5.8 | 0.9 | 44.5 | 3.8 | 0.5 | 8.6 | n.d | n.d | 29.4 | 8.3 | 11.0 | 4.6 | n.d | 43.6 | 3.0 |
| 12 | 2189 | 46.2 | 10.6 | 6.1 | 27.0 | 5.0 | 1.3 | 3.4 | 0.4 | n.d | 25.2 | 20.5 | 20.2 | 10.6 | n.d | 19.6 | 3.8 |
| 13 | 2258 | 48.9 | 8.3 | 3.8 | 29.9 | 4.7 | 0.7 | 3.4 | 0.2 | n.d | 13.3 | 9.2 | 13.6 | 8.1 | n.d | 51.4 | 4.5 |
| 14 | 2318 | 60.7 | 5.2 | 1.7 | 26.5 | 2.6 | n.d | 3.3 | n.d | n.d | 93.7 | 0.7 | 0.8 | n.d | n.d | 4.0 | 0.7 |
| 15 | 2323 | 27.6 | 17.9 | 4.9 | 32.1 | 8.8 | 0.8 | 7.8 | n.d | n.d | 13.7 | n.d | 21.1 | n.d | n.d | 55.6 | 9.6 |
| 16 | 2350 | 71.6 | 8.5 | 4.1 | 10.3 | 0.9 | 1.6 | 2.9 | n.d | n.d | 23.2 | 21.5 | 27.1 | 22.9 | n.d | 5.1 | 0.2 |
| 17 | 2500 | 18.5 | 14.8 | 2.3 | 36.3 | 13.1 | 1.0 | 12.2 | 1.7 | n.d | 13.8 | 0.0 | n.d | n.d | n.d | 75.5 | 10.7 |
| 18 | 2642 | 42.4 | 8.2 | 1.9 | 36.3 | 4.1 | 0.7 | 6.4 | n.d | n.d | 47.5 | 7.7 | 9.6 | 4.3 | n.d | 28.6 | 2.3 |
| 19 | 2705 | 20.2 | 10.4 | 1.1 | 37.1 | 13.5 | 0.8 | 14.9 | 1.8 | 0.2 | 34.9 | 8.4 | 9.9 | 5.7 | n.d | 38.8 | 2.3 |
| 20 | 2846 | 26.9 | 8.1 | 1.3 | 41.8 | 8.8 | 0.9 | 11.4 | 0.6 | n.d | 71.3 | 6.5 | 5.8 | 2.4 | n.d | 13.2 | 1.0 |
| 21 | 2924 | 27.6 | 10.4 | 1.7 | 40.1 | 8.6 | 0.9 | 9.7 | 0.9 | 0.1 | 74.0 | 3.0 | 3.0 | 2.2 | n.d | 16.5 | 1.3 |
| 22 | 3047 | 20.8 | 6.9 | 1.5 | 44.4 | 10.0 | 0.9 | 14.3 | 1.0 | 0.1 | 50.1 | 24.4 | n.d | 2.7 | n.d | 22.1 | 0.6 |
| 23 | 3119 | 24.3 | 8.4 | 3.0 | 39.8 | 10.6 | 1.1 | 11.7 | 1.0 | 0.1 | 28.6 | 8.4 | 12.0 | 7.4 | n.d | 41.5 | 2.2 |
| 24 | 3119 | 42.9 | 1.7 | 0.3 | 45.1 | 1.0 | 0.3 | 8.8 | n.d | n.d | 64.8 | 16.7 | 7.8 | 3.4 | n.d | 7.4 | 0.0 |
| 25 | 3119 | 62.0 | 6.8 | 12.0 | 10.5 | 3.5 | 2.3 | 2.9 | n.d | n.d | 39.2 | 28.3 | 21.7 | 8.3 | n.d | 2.4 | 0.0 |
| 26 | 3160 | 43.0 | 2.5 | 0.8 | 43.3 | 1.4 | 0.7 | 8.4 | n.d | n.d | 26.7 | 11.0 | 15.0 | 4.2 | n.d | 39.4 | 3.7 |
| 27 | 3268 | 45.3 | 1.2 | 0.8 | 37.1 | 1.3 | 1.0 | 10.9 | 2.0 | 0.5 | 40.6 | 16.0 | 13.3 | n.d | n.d | 27.7 | 2.4 |

Acyclic brGDGTs (I, II and III) are generally more abundant than those with cyclopentyl moieties (Table 2). BrGDGTs I and II are the most abundant homologues in all samples. Among the iGDGTs the crenarchaeol and GDGT – 0 are always the most abundant compounds (Table 2). iGDGTs 1 – 3 are present in lower relative abundances.

### *3.2 brGDGT-derived proxies*

MBT, MBT' and CBT were calculated for all the soil samples from the altitudinal transect (Table 3). The CBT ranges from 0.38 to 1.58 (Table 3) and displays no relationship with altitude ($R^2$=0.14, $p$ = 0.12). A cluster of high-altitude soils (>3000 m asl) with high CBT is present. With the exception of this cluster a poor CBT – altitude correlation is still observed ($R^2$=0.23; not shown).

**Table 3: brGDGT and iGDGT-derived proxies as well as temperature and pH estimates derived from these proxies along Mt. Kenya transect.**

| No | Altitude (m asl) | BIT | MBT | MBT' | CBT | pH [17] | pH [1] | MAAT [1] | MAAT [17] | MAAT [34] | MAAT [25] | $TEX_{86}$ | 1302/1292 |
|---|---|---|---|---|---|---|---|---|---|---|---|---|---|
| **1** | 1800 | 0.97 | 0.76 | 0.76 | 1.66 | 4.40 | 4.63 | 15.0 | 16.4 | 17.6 | 14.9 | 0.64 | 1.34 |
| **2** | 1800 | 0.96 | 0.68 | 0.68 | 1.25 | 5.48 | 5.44 | 14.7 | 16.0 | 17.6 | 16.1 | 0.70 | 0.50 |
| **3** | 1823 | 0.88 | 0.62 | 0.62 | 0.76 | 6.77 | 6.41 | 15.6 | 17.7 | 17.5 | 18.6 | 0.77 | 0.44 |
| **4** | 1847 | 0.97 | 0.50 | 0.50 | 0.50 | 7.45 | 6.92 | 13.6 | 14.3 | 17.2 | 17.8 | n.d | 7.00 |
| **5** | 1847 | 0.88 | 0.53 | 0.53 | 0.50 | 7.44 | 6.91 | 14.4 | 15.7 | 17.2 | 18.5 | 0.79 | 0.32 |
| **6** | 1847 | 0.86 | 0.58 | 0.58 | 0.54 | 7.35 | 6.84 | 15.6 | 17.6 | 17.2 | 19.4 | 0.77 | 0.41 |
| **7** | 1897 | 0.68 | 0.69 | 0.69 | 1.32 | 5.30 | 5.31 | 14.8 | 16.1 | 16.9 | 15.9 | 0.84 | 0.46 |
| **8** | 2027 | 0.77 | 0.71 | 0.71 | 1.06 | 5.98 | 5.82 | 16.8 | 19.4 | 16.1 | 18.5 | 0.74 | 0.56 |
| **9** | 2052 | 0.63 | 0.49 | 0.49 | 0.87 | 6.48 | 6.19 | 11.0 | 10.2 | 16.5 | 14.5 | 0.67 | 0.81 |
| **10** | 2097 | 0.64 | 0.64 | 0.64 | 1.17 | 5.69 | 5.60 | 14.2 | 15.0 | 16.2 | 15.8 | n.d | 3.11 |
| **11** | 2130 | 0.65 | 0.51 | 0.51 | 0.86 | 6.51 | 6.22 | 11.7 | 11.3 | 15.7 | 15.0 | 0.74 | 0.45 |
| **12** | 2189 | 0.53 | 0.43 | 0.43 | 0.93 | 6.33 | 6.08 | 8.8 | 6.5 | 15.3 | 12.4 | 0.69 | 0.68 |
| **13** | 2258 | 0.82 | 0.63 | 0.63 | 0.67 | 7.00 | 6.58 | 16.6 | 19.1 | 15.1 | 19.6 | 0.63 | 1.29 |
| **14** | 2318 | 0.79 | 0.61 | 0.61 | 0.78 | 6.70 | 6.36 | 15.3 | 17.1 | 15.1 | 18.2 | 0.74 | 0.26 |
| **15** | 2323 | 0.70 | 0.68 | 0.68 | 1.05 | 6.01 | 5.84 | 15.8 | 17.9 | 14.5 | 17.8 | n.d | 23.20 |
| **16** | 2350 | 0.95 | 0.36 | 0.36 | 0.29 | 7.99 | 7.32 | 10.4 | 9.0 | 14.3 | 15.8 | 1.00 | 0.18 |
| **17** | 2500 | 0.66 | 0.52 | 0.52 | 0.81 | 6.64 | 6.31 | 12.5 | 12.6 | 13.6 | 15.9 | 0.68 | 1.66 |
| **18** | 2642 | 0.63 | 0.32 | 0.32 | 0.38 | 7.76 | 7.15 | 8.7 | 6.2 | 13.2 | 14.1 | 0.68 | 0.90 |
| **19** | 2705 | 0.61 | 0.36 | 0.37 | 0.61 | 7.16 | 6.70 | 8.7 | 6.4 | 12.9 | 13.4 | n.d | 5.42 |
| **20** | 2846 | 0.67 | 0.40 | 0.40 | 0.55 | 7.31 | 6.81 | 10.1 | 8.6 | 12.1 | 14.7 | n.d | 4.47 |
| **21** | 2924 | 0.56 | 0.29 | 0.30 | 0.58 | 7.22 | 6.75 | 6.6 | 3.0 | 11.9 | 11.8 | n.d | 2.26 |
| **22** | 3047 | 0.63 | 0.36 | 0.36 | 0.53 | 7.37 | 6.86 | 9.0 | 6.8 | 11.1 | 13.9 | 0.72 | 0.69 |
| **23** | 3119 | 0.29 | 0.49 | 0.49 | 1.48 | 4.87 | 4.98 | 7.5 | 4.4 | 10.3 | 9.4 | n.d | 3.54 |
| **24** | 3119 | 0.31 | 0.40 | 0.40 | 1.28 | 5.39 | 5.37 | 6.0 | 2.1 | 10.6 | 8.9 | 0.65 | 1.49 |
| **25** | 3119 | 0.23 | 0.45 | 0.45 | 1.53 | 4.74 | 4.89 | 6.1 | 2.1 | 10.6 | 8.1 | n.d | 8.80 |
| **26** | 3160 | 0.31 | 0.46 | 0.46 | 1.35 | 5.21 | 5.24 | 7.5 | 4.4 | 10.5 | 9.9 | 0.68 | 0.68 |
| **27** | 3268 | 0.29 | 0.47 | 0.48 | 1.52 | 4.77 | 4.91 | 7.2 | 3.3 | 10.0 | 8.7 | 0.50 | 1.46 |

**MAAT and pH [17]; corresponds to global temperature and pH calibration [Eqn. 4 and 7, respectively]*
**MAAT and pH [1]; corresponds to global temperature and pH calibration [Eqn. 5 and 8, respectively]*
**MAAT [34]; corresponds to gridded WorldClim global temperature climate dataset; https://worldclim.org/version2*
**MAAT [25]– corresponds to regional temperature calibration [Eqn. 6]*

The reconstructed pH values in acidic to neutral soils display no relation to the elevation. This relationship is similar to those of *in situ* pH measurements from Mt. Kenya [33] and field observations. The soils from the lower elevations (1600 – 2000 m asl) that cover the younger volcanic rocks are mildly acidic to neutral andosol, while the mid altitudes (2000 – 3000 m asl) soils are well drained, moderately deep nitisols (acidic) and those in the high altitudes (>3000 m) are poorly developed, humic nitisols (acidic). The MBT and MBT' values are identical in most cases with the exception of three samples (Table 3). The MBT weakly correlates with altitude ($R^2$ = 0.37, $p$ > 0.001; Figure 3). This is due to the influence of other parameters, especially pH, on this index along Mt. Kenya ($R^2$ = 0.09, $p$ = 0.14,not shown).

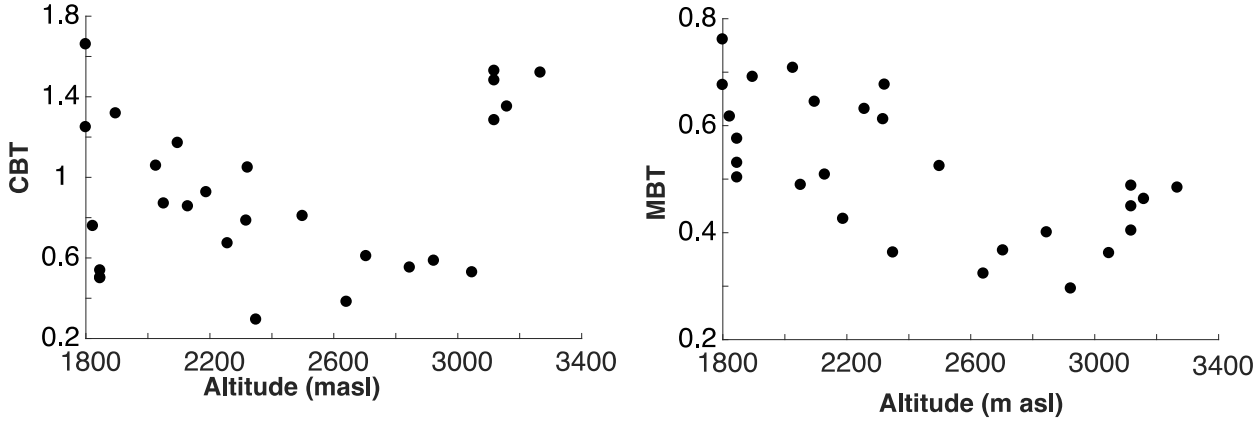


**Figure 3: Relationship between brGDGT-derived indices (MBT/CBT) and altitude.**

MBT/CBT-derived MAAT ranges (Figure 4) from 2.1 °C to 19.4°C, 6.0 °C to 19.4 °C and 8.1 to 19.6 °C using the global soil calibrations by [17] and [1] and the regional calibration by [25], respectively. The MAAT displays a strong linear relationship with altitude (Figure 4). Generally, the MAAT shows a decrease with altitude consistent with previous observations [13], [18], [19] and confirms the fact that brGDGTs can be used as indirect indicators of changes in temperature with altitude. The lapse rate of the reconstructed MAAT are 0.53°C/100 m, 0.90 °C /100 m and 0.42°C /100 based on the [1] [17] [25] calibrations respectively. The comparison of these reconstructed values against the measured temperatures (range10.0 to 17.6 °C; lapse rate of 0.52 °C /100 m) from [34] shows that the estimates from [1] and [25] are closer to the real values than the estimates based on the [17] calibrations (Figure 4).

Although the MBT/CBT correlates with air temperature in East Africa [25], some scatter remains in the relationship, as other environmental parameters, such as soil moisture [35], soil type [36], vegetation [37] or seasonality [31] may also influence the GDGT distribution in soils. As suggested by [25], the application of the brGDGT-derived proxies is site dependent and care has to be taken when applying such proxies to reconstruct past elevation changes.

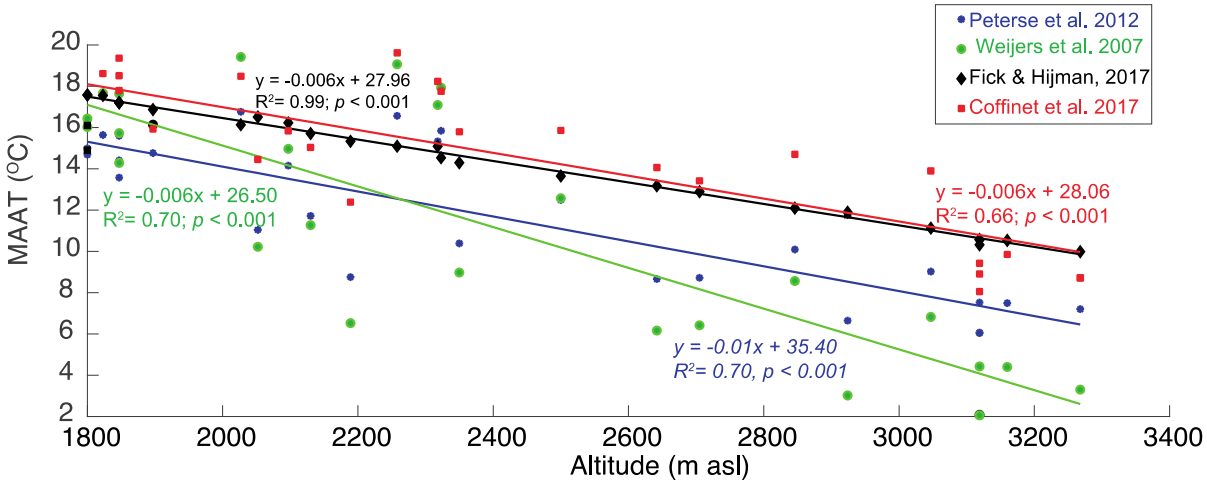


**Figure 4: The reconstructed MAAT from [1], [17] and [25]calibrations. The measured MAAT from Worldclim data [34] is plotted for comparisons along the soil transect.**

### *3.3 iGDGT-derived proxies*

The $TEX_{86}$ was calculated for Mt. Kenya soil samples. A proper application of $TEX_{86}$ requires that the iGDGTs present in the samples are mainly derived from *Thaumarchaeota* [10]. A value of caldarchaeol (GDGT-I) vs. crenarchaeol ratio higher than 2 is considered as an indication of the predominance of methanogenic Archaea [16]. Reliable $TEX_{86}$ values can only be obtained when *Thaumarchaeota* are the most abundant (i.e. the GDGT-I vs. GDGT-VI ratio is lower than 2). In our soil samples the GDGT – 0/ Crenarchaeol ratio is much lower than 2 (0.4 to 1.6) in 23 out of 31 samples (Table 3). The calculation of the $TEX_{86}$ was achieved only for the samples presenting a GDGT-0/crenarchaeol ratio lower than 2 (Table 3). This index displayed a weak relationship with altitude ($R^2$ = 0.28, $p$ = 0.03), questioning, its applicability as a palaeoelevation proxy along Mt. Kenya (Figure 5). In contrast, a stronger correlation was obtained from a shorter transect (500-2500 m) along Mt. Rungwe ($R^2$ 0.50; [20]) and from a higher altitude transect (3250-4000 m) along Mt. Xiangpi ($R^2$ 0.68; [3]).

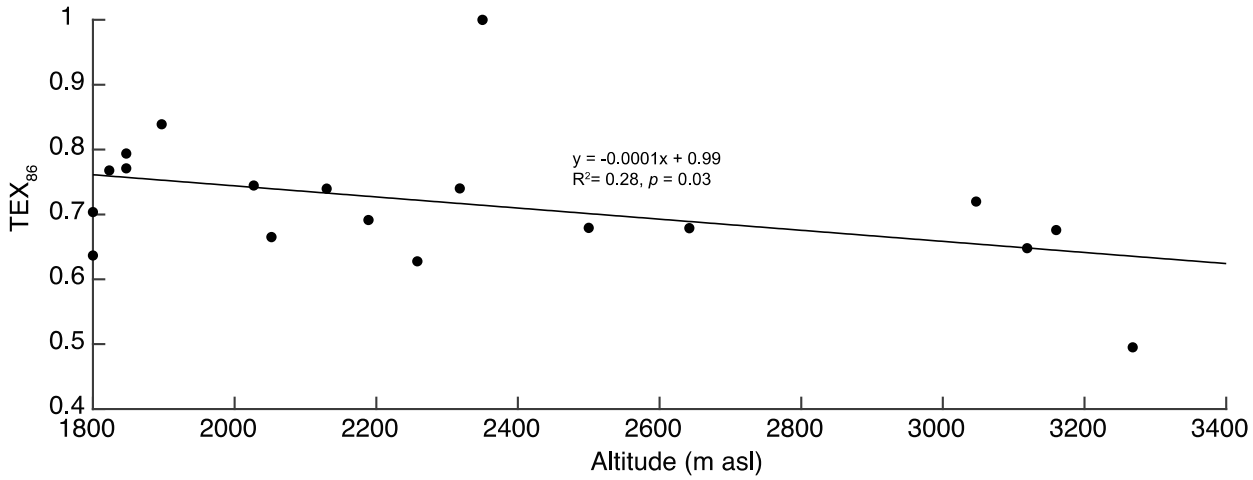


**Figure 5: The $TEX_{86}$ reconstruction along the transect.**

In addition to temperature, unique environmental parameters, such as vegetation cover, precipitation and soil humidity could also have an effect on the distribution of the iGDGTs and by extension affect the $TEX_{86}$ values obtained. Soil humidity was notably suggested to have an influence on brGDGT [1], [38] and iGDGT [39] distributions in soils. Along Mt. Kenya, the topography enhances

the effects of the precipitation received during the rainy season [29]. The amount of precipitation gradually increases with altitude until about 2000 – 2500 m asl after which a decline in rainfall similar to other East African mountains is observed [26], [28]. Precipitation will have an impact on the soil moisture content as can be seen in the well-developed well drained soils between 2000 – 2500 m and the poorly developed soils above this altitude. This is in contrast to Mt. Rungwe where the precipitation amount does not change significantly with altitude [20], which could explain the stronger relationship between $TEX_{86}$ and temperature along this mountain. Similarly, the larger scatter observed by [25] in the relationship between $\delta^2$Hwax and altitude along Mt. Kenya than along Mt. Rungwe could also be explained by precipitation changes observed in the ecological zones that correspond to specific altitude. In our study, the from 1800 – 2500m asl are a mix of $C_3/C_4$ vegetation type while those >2500m asl are $C_3$ - type [39]. Thus, despite the varied species along the transect, it is possible to assume that precipitation plays a key role in the changes observed in the $\delta^2$Hwax. Additional regional studies on the applicability of $TEX_{86}$ as a temperature proxy are needed along other altitudinal transects.

In contrast with the MBT/CBT, the applicability of $TEX_{86}$ as a temperature proxy in soils has been much less investigated. Studies along altitudinal transects in China [3] and Tanzania [20] reported a linear relationship between $TEX_{86}$ and altitude, implying that air temperature could have an effect on the distribution of iGDGTs in soils. Nevertheless, a large degree of scatter between these two independent altitudinal gradients was observed, implying that additional studies are needed to fully understand the factors impacting on the potential application of $TEX_{86}$ as a paleoelevation proxy.

## 4. Conclusions

The brGDGT distribution was shown to vary with elevation in soils from Mt. Kenya, as reflected in the decrease in MBT/CBT-derived MAAT with altitude. The MBT/CBT-derived temperature lapse rate as well as absolute temperature range calculated using the global soil calibration by [1] was similar to values derived from *in situ* measurements by [34]. This confirms the robustness of the MBT/CBT proxy in East Africa. The $TEX_{86}$ displayed a weak correlation with altitude and a large degree of scatter in contrast with some previous studies along Tanzanian or Chinese mountains. This could be explained by the fact that other parameters than temperature, such as precipitation/soil humidity locally influence the distribution of iGDGTs and thus $TEX_{86}$ values. A better understanding of environmental parameters affecting iGDGT distribution regionally is required before a potential application of the $TEX_{86}$ as a paleoelevation proxy along individual mountains.

## Acknowledgments

The authors would like to thank Dr. Sylvie Derenne and Dr. Christelle Anquetil for their assistance at the lab. The work under was carried out under permit NCST/RCD/17/013/02 on Mt. Kenya (C. Omuombo) supported by French IRD and Campus France through the French Embassy in Nairobi.

## References


[1] Peterse, F., van der Meer, J., Schouten, S., Weijers, J. W. H., Fierer, N., Jackson, R. B., Kim and J-H. Sinninghe Damsté, J. S. (2012) Revised calibration of the MBT–CBT paleotemperature proxy based on branched tetraether membrane lipids in surface soils. Geochimica et Cosmochimica Acta, **96**: 215-229. DOI: 10.1016/j.gca.2012.08.011.

[2] Schouten, S., Rijpstra, W.I.C., Durisch-Kaiser, E., Schubert, C.J. and Sinninghe Damsté, J.S. (2012) Distribution of glycerol dialkyl glycerol tetraether lipids in the water column of Lake Tanganyika. Organic Geochemistry, **53**: 34-37.

[3] Liu, W., Wang, H., Zhang, C.L., Liu, Z. and He, Y. (2013) Distribution of glycerol dialkyl glycerol tetraether lipids along an altitudinal transect on Mt. Xiangpi, NE Qinghai-Tibetan Plateau, China. Organic Geochemistry, **57** (C): 76-83.

[4] Weijers, J.W.H., Schouten, S., Van den Donker, J.C., Hopmans, E.C. and Sinninghe Damsté, J.S. (2007) Environmental controls on bacterial tetraether membrane lipid distribution in soils. Geochimica et Cosmochimica Acta, **71** (3): 703-713. DOI:10.1016/j.gca.2006.10.003.

[5] Sinninghe Damsté, J. S., Hopmans, E. C., Pancost, R. D., Schouten, S. and Geenevasen, J. A. J. (2000) Newly discovered non-isoprenoid glycerol dialkyl glycerol tetraether lipids in sediments. Chemical Communications, **17**: 1683-1684. DOI:10.1039/B004517I.

[6] Huguet, A., Fosse, C., Laggoun-Défarge, F., Toussaint, M. L. and Derenne, S. (2010) Occurrence and distribution of glycerol dialkyl glycerol tetraethers in a French peat bog. Organic Geochemistry, **41** (6): 559-572. DOI:10.1016/j.orggeochem.2010.02.015.

[7] Buckles, L.K., Weijers, J.W.H., Verschuren, D. and Sinninghe Damste, J.S. (2014) Sources of core and intact branched tetraether membrane lipids in the lacustrine environment: Anatomy of Lake Challa and its catchment, equatorial East Africa. *Geochimica et Cosmochimica Acta,* **140**: 106-126. DOI:10.1016/j.gca.2014.04.042.

[8] Yang, H., Ding, W., Zhang, C.L., Wu, X., Ma, X., He, G., Huang, J. and Xie, S. (2011) Occurrence of tetraether lipids in stalagmites: Implications for sources and GDGT-based proxies. Organic Geochemistry, **42**: 108-115.

[9] Pearson, A. and Ingalls, A.E. (2013) Assessing the Use of Archaeal Lipids as Marine Environmental Proxies. Annual Review of Earth and Planetary Sciences, **41**: 359-384.

[10] Sinninghe Damste, J.S., Ossebaar, J., Schouten, S. and Verschuren, D. (2012) Distribution of tetraether lipids in the 25-ka sedimentary record of Lake Challa: extracting reliable $TEX_{86}$ and MBT/CBT palaeotemperatures from an equatorial African lake. Quaternary Science Reviews, **50**: 43-54. DOI:10.1016/j.quascirev.2012.07.001.

[11] Schouten, S., Hopmans, E.C. and Sinninghe Damsté, J.S. (2013) The organic geochemistry of glycerol dialkyl glycerol tetraethers: a review. Organic Geochemistry, **54**: 19-61.

[12] Schouten, S., Hopmans, E.C., Schefuß, E. and Sinninghe Damste, J.S. (2002) Distributional variations in marine crenarchaeotal membrane lipids: a new tool for reconstructing ancient sea water temperatures? Earth and Planetary Science Letters, **204**: 265-274.

[13] Weijers, J.W.H., Schouten, S., Spaargaren, O.C. and Sinninghe Damsté, J.S. (2006) Occurrence and distribution of tetraether membrane lipids in soils: Implications for the use of the TEX86 proxy and the BIT index. Organic Geochemistry, **37** (12): 1680-1693. DOI:10.1016/j.orggeochem.2006.07.018.

[14] Weijers, J.W.H., Panoto, E., van Bleijswijk, J., Schouten, S., Rijpstra, W.I.C., Balk, M., Stams, A.J.M. and Sinninghe Damsté, J.S. (2009) Constraints on the Biological Source(s) of the Orphan Branched Tetraether Membrane Lipids. Geomicrobiology Journal, **26**: 402-414.

[15] Hopmans, E.C., Weijers, J.W., Schefuß, E., Herfort, L., Sinninghe Damsté, J.S. and Schouten, S. (2004) A novel proxy for terrestrial organic matter in sediments based on branched and isoprenoid tetraether lipids. Earth and Planetary Science Letters, **224**: 107-116.

[16] Blaga, C. I., Reichart, G. J., Heiri, O. and Sinninghe Damsté, J. S. (2009) Tetraether membrane lipid distributions in water-column particulate matter and sediments: a study of 47 European lakes along a north–south transect. Journal of Paleolimnology, **41** (3): 523-540. DOI:10.1007/s10933-008-9242-2.

[17] Weijers, J.W.H., Schouten, S., Van den Donker, J.C., Hopmans, E.C. and Sinninghe Damsté, J.S. (2007) Environmental controls on bacterial tetraether membrane lipid distribution in soils. Geochimica et Cosmochimica Acta, **71** (3): 703-713. DOI:10.1016/j.gca.2006.10.003.

[18] Sinninghe Damsté, J.S., Ossebaar, J., Schouten, S. and Verschuren, D. (2008) Altitudinal shifts in the branched tetraether lipid distribution in soil from Mt. Kilimanjaro (Tanzania): Implications for the MBT/CBT continental palaeothermometer. Organic Geochemistry, **39**: 1072-1076.

[19] Peterse, F., Kim, J-H., Schouten, S., Kristensen, D. K., Koç, N. and Sinninghe Damsté, J. S. (2009) Constraints on the application of the MBT/CBT palaeothermometer at high latitude environments (Svalbard, Norway). Organic Geochemistry, **40** (6): 692-699. DOI:10.1016/j.orggeochem.2009.03.004.

[20] Ernst, N., Peterse, F., Breitenbach, S.F.M., Syiemlieh, H.J. and Eglinton, T.I. (2013) Biomarkers record environmental changes along an altitudinal transect in the wettest place on Earth. Organic Geochemistry, **60**: 93-99.

[21] Coffinet, S., Huguet, A., Williamson, D., Fosse, C. and Derenne, S. (2014) Potential of GDGTs as a temperature proxy along an altitudinal transect at Mount Rungwe (Tanzania). Organic Geochemistry, **68**: 82-89.

[22] Tierney, J.E. and Russell, J.M. (2009) Distributions of branched GDGTs in a tropical lake system: Implications for lacustrine application of the MBT/CBT paleoproxy. Organic Geochemistry, **40** (9): 1032-1036.
[23] Weijers, J. W. H., Steinmann, P., Hopmans, E. C., Schouten, S. and Sinninghe Damsté, J.S. (2011) Bacterial tetraether membrane lipids in peat and coal: Testing the MBT-CBT temperature proxy for climate reconstruction. Organic Geochemistry, **42** (5): 477-486. DOI:10.1016/j.orggeochem.2011.03.013.
[24] De Jonge, C., Hopmans, E.C., Zell, C.I., Kim, J.-H., Schouten, S. and Sinninghe Damsté, J.S. (2014) Occurrence and abundance of 6-methyl branched glycerol dialkyl glycerol tetraethers in soils: Implications for palaeoclimate reconstruction. *Geochimica et Cosmochimica Acta,* **141**: 97-112.
[25] Coffinet, S., Huguet, A., Pedentchouk, N., Bergonzini, L., Omuombo, C., Williamson, D., Anquetil, C., Jones, M., Majule, A., Wagner, T. and Derenne, S. (2017) Evaluation of branched GDGTs and leaf wax n-alkane $\delta^2H$ as (paleo) environmental proxies in East Africa. *Geochimica et Cosmochimica Acta,* **198**: 182-193. DOI:10.1016/j.gca.2016.11.020.
[26] Coe, M.J. (1967) The ecology of the Alpine zone of Mount Kenya. Dr. W. Junk Publishers, The Hague, 136pp.
[27] Hamilton, A.C. (1982) Environmental History of East Africa: A Study of the Quaternary. Academic Press, London, 328pp.
[28] Camberlin, P., Moron, V., Okoola, R., Philippon, N. and Gitau, W. (2009) Components of rainy seasons' variability in Equatorial East Africa: onset, cessation, rainfall frequency and intensity. Theoretical and Applied Climatology, **98**: 237-249.
[29] Camberlin, P., Boyard-Micheau, J., Philippon, N., Baron, C., Leclerc, C. and Mwongera, C. (2012) Climatic gradients along the windward slopes of Mount Kenya and their implication for crop risks. Part 1: climate variability. International Journal of Climatology, **34**:2136-2152. DOI: 10.1002/joc.3427.
[30] Thompson, B.W. (1965) Climate of Africa. Oxford University Press, London and Nairobi, 132pp.
[31] Huguet, A., Fosse, C., Laggoun-Défarge, F., Delarue, F. and Derenne, S. (2013) Effects of a short-term experimental microclimate warming on the abundance and distribution of branched GDGTs in a French peatland. Geochimica et Cosmochimica Acta, **105**: 294-315.
[32] Loomis, S.E., Russell, J.M. and Sinninghe Damsté, J.S. (2011) Distributions of branched GDGTs in soils and lake sediments from western Uganda: Implications for a lacustrine paleothermometer. Organic Geochemistry, **42**: 739-751.
[33] Dijkshoorn J.A, Macharia PN, Huting J.R.M and Njoroge C.R.K (2010) Soil and Terrain Database for the Upper Tana, Kenya. Green Water Credits Report 11, ISRIC – World Soil Information, Wageningen pp 47.
[34] Fick, S.E. and Hijman, R.J. (2017) Worldclim 2: New 1-km spatial resolution climate. http://worldclim.org/version2.
[35] Menges, J., Huguet, C., Alcañiz, J. M., Fietz, S., Sachse, D. and Rosell-Melé, A. (2014) Influence of water availability in the distributions of branched glycerol dialkyl glycerol tetraether in soils of the Iberian Peninsula. Biogeosciences, **11**: 2571-2581.
[36] Davtian, N., Ménot, G., Bard, E., Poulenard, J. and Podwojewski (2016) Consideration of soil types for the calibration of molecular proxies for soil pH and temperature using global soil datasets and Vietnamese soil profiles. Organic Geochemistry, **101**: 140-153.
[37] Liang, J., Russell, J., Xie, H., Lupien, R., Si, G., Wang, J., Hou, J. and Zhang, G. (2018) Vegetation effects on temperature calibrations of branched glycerol dialkyl glycerol tetraether (brGDGTs) in soils. Organic Geochemistry, **127**: 1-11.
[38] Dirghangi, S.S., Pagani, M., Hren, M.T. and Tipple, B.J. (2013) Distribution of glycerol dialkyl glycerol tetraethers in soils from two environmental transects in the USA. Organic Geochemistry, **59**: 49-60.
[39] Wang, H., Liu, W., Zhang, C.L., Wang, Z., Wang, J., Liu, Z. and Dong, H. (2012) Distribution of glycerol dialkyl glycerol tetraethers in surface sediments of Lake Qinghai and surrounding soil. Organic Geochemistry, **47**: 78-87.
[40] Omuombo, C.A (2020) Biogeochemical proxies of climate change in the central Kenya highlands. DPhil thesis unpublished, University of Nairobi.